Two-Dimensional Transmit Beamforming for MIMO Radar with Sparse Symmetric Arrays

Aboulnasr Hassanien, Matthew W. Morency, Arash Khabbazibasmenj, Sergiy A. Vorobyov
Dept. of Electrical and Computer Engineering
University of Alberta
Edmonton, AB, T6G 2V4, Canada
{hassanie,morency}@ualberta.ca
{khabbazi,svorobyo}@ualberta.ca

Joon-Young Park
Samsung Thales Co., Ltd.
Core Technology Group
Chang-Li 304, Namsa-Myun
Cheoin-Gu, Yongin-City
Gyeonggi-D, Korea 449-885
jy97.park@samsung.com

Seon-Joo Kim
Agency of Defense Development
The 3rd R&D Institute
Daejeon-City, Korea 305-600
sjkim@add.re.kr

Abstract— **Multiple-input multiple-output (MIMO) radar using one-dimensional transmit arrays has been thoroughly investigated in the literature. In this paper, we consider the MIMO radar problem in the context of two-dimensional (2D) transmit arrays. In particular, we address the problem of transmit beamforming design using 2D arrays with symmetrically missing elements. This situation is encountered in practice when some of the array elements are assigned for a different purpose, e.g., for communication purposes. We cast the transmit beamforming problem as an optimization problem that minimizes the difference between a desired transmit beampattern and the actual one while satisfying constraints such as uniform transmit power across the array elements, sidelobe level control, etc. Moreover, different transmit beams can be enforced to have rotational invariance with respect to each other, a property that enables efficient computationally cheap 2D direction finding at the receiver. Semi-definite relaxation is used to recast the optimization problem as a convex one that can be solved efficiently using the interior point optimization methods. Simulations are used to validate the proposed method.**

I. Introduction and Motivation

The emerging concept of multiple-input multiple-output (MIMO) radar has been the focus of intensive research [1]–[3]. Many researchers focussed their research on MIMO radar with widely separated antennas capitalizing on the spatial diversity of the target [2], [4], [5]. It has been shown in the literature that the aforementioned type of MIMO radar improves the target detection performance, enhances the ability to combat signal scintillation, and enables accurate parameter estimation of rapidly moving targets [4], [5]. Other researchers investigated MIMO radar based on colocated transmit/receive arrays and showed that the latter type of MIMO radar enables improving angular resolution, increasing the upper limit on the number of detectable targets, improving parameter identifiability, and extending the array aperture by virtual sensors [3], [6]–[8]. However, MIMO radar suffers from the loss of coherent transmit processing gain as a result of omnidirectional transmission of orthogonal waveforms at the transmitter.

Several approaches for transmit beamforming in MIMO radar with colocated transmit arrays have been investigated in the literature [6]–[13]. The aforementioned methods have been developed in the context of one-dimensional transmit arrays. It has been shown in [8] that the performance of a MIMO radar system with a number of waveforms less than the number of transmit antennas associated with using transmit beamforming gain is better than the performance of a MIMO radar system with full waveform diversity with no transmit beamforming gain. This fact becomes more evident in the case when the transmit array contains a large number of antennas, e.g., in the case of two-dimensional (2D) transmit arrays. Beyond transmit preprocessing gain, transmit beamforming can offer other advantages. By designing the transmit beamforming matrix, it is possible to enforce properties such as the rotational invariance property (hereafter denoted as RIP), and uniform transmit power among waveforms. By enforcing the RIP, we can improve the performance of DOA estimation, as well as enable low complexity, search free direction finding methods to be used at the receiver [8], [11]. Enforcing even power across all transmitted waveforms also improves the performance of DOA estimation algorithms. Finally, not only it is possible to enforce these properties, but also, it separates the problem of beamforming entirely from that of waveform design. As a result, the only restriction we place on our set of waveforms is that they be orthogonal.

In this paper, we consider the problem of transmit beamforming for MIMO radar with 2D planar arrays. Practical considerations sometimes mandate that some elements of the array be assigned for a different purpose other than beamforming, e.g., for communication purposes. Therefore, we assume that the MIMO radar is equipped with 2D planar transmit array with a symmetric shape with respect to both the x- and y-axes in a cartesian coordinates. Examples of such arrays are the uniform rectangular array (URA) and the uniform rectangular frame array (URFA) shown in Figs. 1a and 1b, respectively. Other examples for symmetric 2D planar arrays with dual invariance structure are shown in Figs. 1c and 1d. We formulate the 2D transmit beamforming problem based on minimizing the difference between a desired 2D beampattern and the actual one while satisfying the requirement of uniform power distribution across the transmit array elements. It is also possible to have uniform power distribution over individual transmit waveforms. We also enforce the rotational

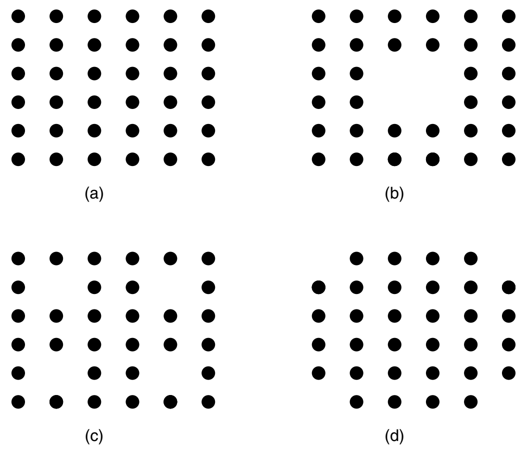

Fig. 1. Symmetric planar array configurations: (a) Uniform rectangular array (URA); (b) Uniform rectangular frame array (URFA); (c) Symmetric array with dual invariance structure; (d) URA with no elements at corners.

invariance property (RIP) between different transmit beams, i.e., we enforce the condition that two transmit beams have exactly the same magnitude but differ in phase. The resulting optimization problem is non-convex. Therefore, we use semi-definite relaxation to recast it as a convex one and solve it using semi-definite programming. We use simulation examples to validate our proposed 2D transmit beamforming method.

II. System Model

Consider a mono-static radar system with a transmit array being an $M_t \times N_t$-antenna uniform rectangular array (URA), where M_t is the number of antenna elements in a given column and N_t is the number of antenna elements in a given row, and a receive array being an M_r-antenna planar array with an arbitrary structure. The model we derive hereafter for the URA can be straightforwardly applied to other symmetric arrays shown in Fig. 1 with small modification. The elements on any given column in the transmit array are assumed to be equally spaced with interelement spacing d_x while the interelement spacing between any two adjacent elements on any row is given by d_y. Let the $M_tN_t \times 1$ steering vector of the transmit array be represented as

$$\mathbf{a}(\theta,\phi) = \mathrm{vec}\left(\mathbf{Z} \odot [\mathbf{u}(\theta,\phi)\mathbf{v}^T(\theta,\phi)]\right) \tag{1}$$

where $\mathbf{Z}$ is an $M_t \times N_t$ matrix of ones and zeros where the mn-th entry equals zero if the mn-th element of the array is absent, $\mathrm{vec}(\cdot)$ stands for the operator that stacks the columns of a matrix in one column vector, $(\cdot)^T$ denotes the transpose, $\odot$ stands for the Hadamard product, θ and ϕ denote the elevation and azimuth angles, respectively, and $\mathbf{u}$ and $\mathbf{v}$ are vectors of dimension $M_t \times 1$ and $N_t \times 1$, respectively, that are defined as follows

$$\mathbf{u}(\theta,\phi)=\left[1, e^{j2\pi d_x \sin\theta\cos\phi}, \ldots, e^{j2\pi(M_t-1)d_x \sin\theta\cos\phi}\right]^T \tag{2}$$

$$\mathbf{v}(\theta,\phi)=\left[1, e^{j2\pi d_y \sin\theta\sin\phi}, \ldots, e^{j2\pi(N_t-1)d_y \sin\theta\sin\phi}\right]^T. \tag{3}$$

We are interested in focusing the transmit energy into a 2D spatial sector defined by $\Theta = [\theta_1 \;\; \theta_2]$ in the elevation domain and $\Phi = [\phi_1 \;\; \phi_2]$ in the azimuth domain. In the mean time, we wish to restrict the transmit power to be uniform across the transmit array elements and to enforce the RIP at the transmit array. Let $\boldsymbol{\psi}(t) = [\psi_1(t), \ldots, \psi_K(t)]$ be the $K \times 1$ vector of predesigned independent waveforms which satisfy the orthogonality condition $\int_T \boldsymbol{\psi}(t)\boldsymbol{\psi}^H(t) = \mathbf{I}_K$, where T is the radar pulse duration, $\mathbf{I}_K$ is the identity matrix of size K, and $(\cdot)^H$ stands for the Hermitian transpose.

The transmit energy focusing can be achieved by forming K transmit beams where each of the orthogonal waveforms is radiated over one beam. Following the guidance of [8], the optimal number of transmit beams K can be taken as the number of effective eigenvalues of the following semi-definite matrix

$$\mathbf{A}(\theta,\phi) = \int_\Theta \int_\Phi \mathbf{a}(\theta,\phi)\mathbf{a}^H(\theta,\phi) d\phi d\theta. \tag{4}$$

It is worth noting that usually $K \ll M_tN_t$ holds especially when M_t and N_t are large.

The $M_tN_t \times 1$ vector that contains the complex envelope (i.e., the baseband representation) of the transmit signals that should be fed to the transmit antennas can be modeled as

$$\mathbf{s}(t) = \sum_{k=1}^{K} \mathbf{w}_k \psi_k(t) \tag{5}$$

where $\mathbf{w}_k$ is the $M_tN_t \times 1$ transmit weight vector used to form the kth transmit beam. The array transmit beampattern can be written as

$$\begin{aligned} P(\theta,\phi) &= \mathbf{a}^H(\theta,\phi)\left(\int_T \mathbf{s}(t)\mathbf{s}^H(t)dt\right)\mathbf{a}(\theta,\phi) \\ &= \sum_{k=1}^{K} \mathbf{a}^H(\theta,\phi)\mathbf{w}_k\mathbf{w}_k^H\mathbf{a}(\theta,\phi) \\ &= \|\mathbf{W}^H\mathbf{a}(\theta,\phi)\|^2 \end{aligned} \tag{6}$$

where $\|\cdot\|$ denotes the Euclidian norm of a vector and $\mathbf{W} \triangleq [\mathbf{w}_1, \ldots, \mathbf{w}_K]$ is the $M_tN_t \times K$ transmit beamforming weight matrix.

Assuming that L targets are present in a certain Doppler-range bin, the $M_r \times 1$ receive array observation vector can be written as

$$\mathbf{x}(t,\tau)=\sum_{l=1}^{L} \beta_l(\tau)\mathbf{b}(\theta_l,\phi_l)\left(\mathbf{W}^H\mathbf{a}(\theta_l,\phi_l)\right)^H\boldsymbol{\psi}(t)+\mathbf{z}(t,\tau) \tag{7}$$

where t and τ are the fast and slow time indexes, respectively, $\mathbf{b}(\theta,\phi)$ is the $M_r \times 1$ steering vector of the receive array, $\beta(\theta_l,\phi_l)$ is the reflection coefficient associated with the lth target with variance σ_β^2, and $\mathbf{z}(t,\tau)$ is the $M_r \times 1$ vector of zero-mean white Gaussian noise with variance σ_z^2. We assume that the reflection coefficients obey the Swerling II target model, i.e., they remain constant within the whole duration of the radar pulse but change from pulse to pulse. The receive array observation vector $\mathbf{x}(t,\tau)$ is matched-filtered to each of the orthogonal basis waveforms $\psi_k(t), k = 1, \ldots, K$, producing the $M_r \times 1$ virtual data vectors

$$\begin{aligned}\mathbf{y}_k(\tau) &= \int_{\mathrm{T}} \mathbf{x}(t,\tau)\psi_k^*(t)dt \\ &= \sum_{l=1}^{L} \beta_l(\tau)\left(\mathbf{w}_k^H \mathbf{a}(\theta_l,\phi_l)\right)^* \mathbf{b}(\theta_l,\phi_l) + \mathbf{z}_k(\tau) \quad (8)\end{aligned}$$

where $\mathbf{z}_k(\tau) \triangleq \int_{\mathrm{T}} \mathbf{z}(t,\tau)\psi_k^*(t)dt$ is the $M_r \times 1$ noise term whose covariance is $\sigma_z^2 \mathbf{I}_{M_r}$ and $(\cdot)^*$ stands for the conjugation. Note that $\mathbf{z}_k(\tau)$ and $\mathbf{z}_{k'}(\tau)$ $(k \neq k')$ are independent due to the orthogonality between $\psi_k(t)$ and $\psi_{k'}(t)$.

In the following section, we develop a method for 2D transmit beamforming design and show how to solve the associated optimization problem using semidefinite relaxation techniques [16], [17]. We also show how to enforce the 2D RIP at the transmit side of the MIMO radar while designing the transmit beamforming.

III. 2D Transmit Beamspace design

We design the 2D transmit beamforming based on the minimum error criterion, i.e, by minimizing the difference between a desired 2D transmit beampattern and the actual beampattern given by (6). Meanwhile, we wish to have uniform power distribution across the transmit array elements. Therefore, the design problem can be formulated as the following constrained optimization problem

$$\min_{\mathbf{w}_1,\ldots,\mathbf{w}_K} \max_{\theta,\phi} \left| P_d(\theta,\phi) - \sum_{k=1}^{K} \mathbf{w}_k^H \mathbf{a}(\theta,\phi)\mathbf{a}^H(\theta,\phi)\mathbf{w}_k \right| \quad (9)$$

$$\text{s.t.} \quad \sum_{k=1}^{K} \left|\mathbf{W}_{[lk]}\right|^2 = \frac{E}{M_t N_t}, \quad l = 1, \cdots, M_t N_t \quad (10)$$

where $P_d(\theta,\phi)$ is the desired beampattern, $\mathbf{W}_{[lk]}$ denotes the element located at the lth row and kth column of $\mathbf{W}$, and E is the total amount of power available. In the case where we have missing elements, these elements still draw power for communications purposes in our model. As such, the power per antenna should remain unchanged from the fully populated case. The constraint (10) in this case can be interpreted as an average power criterion. However, our model only requires that our signals $\boldsymbol{\psi}(t)$ be orthogonal. As such, this constraint does not preclude using signals which have a constant envelope. Rather, this optimization problem specifies the constraint against which we must design our signals to have constant envelope, namely, that the instantaneous power per symbol per antenna of the designed signal must not exceed $E/M_t N_t$. As a constant envelope signal has a unit peak to average power ratio, this will ensure that the constraint (10) can be obeyed without clipping. While the problem of designing such signal sets is not a trivial one, it is indeed separate from our optimization problem. Other conditions can also be enforced such as equal power between orthogonal waveforms, and coherent power addition between waveforms within a given sector. Indeed, these problems become important for 2D target localization DOA estimation performance. We do not, however, investigate these problems in this paper. The optimization problem (9)–(10) is a non-convex quadratically constrained quadratic programming (QCQP) problem which is, in general, not easy to solve in a computationally efficient manner. Therefore, we use the semidefinite relaxation technique [16], [17] to recast it as a convex one. Introducing the new variables $\mathbf{X}_k = \mathbf{w}_k\mathbf{w}_k^H, \ k = 1, \ldots, K$, the optimization problem (9)–(10) can be reformulated as

$$\min_{\mathbf{X}_1,\ldots,\mathbf{X}_K} \max_{\theta,\phi} \left| P_d(\theta,\phi) - \sum_{i=1}^{K} \mathrm{Tr}\{\mathbf{a}(\theta,\phi)\mathbf{a}^H(\theta,\phi)\mathbf{X}_k\} \right| \quad (11)$$

$$\text{s.t.} \quad \sum_{k=1}^{K} \mathrm{diag}\{\mathbf{X}_k\} = \frac{E}{M_t N_t}\mathbf{1}_{M_t N_t \times 1} \quad (12)$$

$$\mathrm{rank}(\mathbf{X}_k) = 1, \quad k = 1, \ldots, K \quad (13)$$

where $\mathrm{Tr}\{\cdot\}$ and $\mathrm{diag}\{\cdot\}$ denote the trace and the diagonal of a square matrix, respectively, $\mathbf{1}_{M_t N_t \times 1}$ is the $M_t N_t \times 1$ vector of all ones, and $\mathrm{rank}(\cdot)$ denotes the rank of a matrix. The optimization problem (11)–(13) remains non-convex due to the rank constraint in (13). Therefore, we use the semidefinite relaxation technique [14]– [17] to recast it as a convex one. By relaxing the rank constraint, the problem (11)–(13) can be reformulated as

$$\min_{\mathbf{X}_1,\ldots,\mathbf{X}_K} \max_{\theta,\phi} \left| P_d(\theta,\phi) - \sum_{i=1}^{K} \mathrm{Tr}\{\mathbf{a}(\theta,\phi)\mathbf{a}^H(\theta,\phi)\mathbf{X}_k\} \right| \quad (14)$$

$$\text{s.t.} \quad \sum_{k=1}^{K} \mathrm{diag}\{\mathbf{X}_k\} = \frac{E}{M_t N_t}\mathbf{1}_{M_t N_t \times 1} \quad (15)$$

$$\mathbf{X}_k \succeq 0, \quad k = 1, \ldots, K. \quad (16)$$

The optimization problem (14)–(16) can be solved in polynomial time using available optimization techniques, e.g., the interior point methods (see [16], [17] and references therein). In order to explain how the solution of the problem (9)–(10) is extracted, let us consider the optimal solution of the relaxed problem (14)–(16) denoted as $\mathbf{X}_k^{opt}, k = 1, \cdots, K$. The optimal $\mathbf{w}_k$ is simply the principal eigenvector of $\mathbf{X}_k^{opt}$ if the rank of $\mathbf{X}_k^{opt}$ is equal to one. However, if the corresponding rank is greater than one, we need to resort to randomization techniques to extract the optimal solution. A number of different randomization techniques have been developed in the literature [16]. Briefly, the essence of such techniques is to generate first a set of candidate vectors and then choose the best vector among all candidate vectors.

To explain the randomization technique used in this paper, let us consider the eigen value decomposition of $\mathbf{X}_k^{opt}$ as $\mathbf{X}_k^{opt} = \mathbf{U}_k\mathbf{\Sigma}_k\mathbf{U}_k^H$. We choose the lth candidate vector for $\mathbf{w}_k$ as $\mathbf{w}_k^{can,l} = \mathbf{U}_k\mathbf{\Sigma}_k^{1/2}\mathbf{v}_k^l$ where $\mathbf{v}_k^l$ is a random vector with elements uniformly distributed on the unit circle of the complex plane. After choosing the lth set of random vectors, if the constraint that each element of the vector $\sum_{k=1}^{K} \mathrm{diag}\{\mathbf{w}_k^{can,l}(\mathbf{w}_k^{can,l})^H\}$ equals $E/(M_t N_t)$ does not hold, we simply map the resulting random vectors to a nearby feasible point by scaling the ith element of each candidate vector $\mathbf{w}_k^{can,l}$ so that the aforementioned constraint is satisfied. Then, from the set of all candidate vectors we select the best one which minimizes the objective function, i.e., we select the set of vectors for which $\max_{\theta,\phi} |P_d(\theta,\phi) - \sum_{k=1}^{K} (\mathbf{w}_k^{can,l})^H \mathbf{a}(\theta,\phi)\mathbf{a}^H(\theta,\phi)\mathbf{w}_k^{can,l}|$ has minimum value.

A. Enforcing the RIP

The steering vector expression (1) of any symmetric 2D array can be rewritten as

$$\begin{aligned} \mathbf{a}(\theta,\phi) &= [\mathbf{z}_1{}^T \odot \mathbf{u}_1^T(\theta,\phi), \ldots, \mathbf{z}_{N_t}{}^T \odot \mathbf{u}_{N_t}^T(\theta,\phi)]^T \\ &= [\mathbf{a}_1^T(\theta,\phi), \ldots, \mathbf{a}_{N_t}^T(\theta,\phi)]^T \end{aligned} \tag{17}$$

where $\mathbf{a}_n(\theta,\phi) \triangleq \mathbf{z}_1 \odot \mathbf{u}_n(\theta,\phi)$, $n = 1, \ldots, N_t$, $\mathbf{u}_n(\theta,\phi) = e^{j\mu_n(\theta,\phi)}\mathbf{u}(\theta,\phi)$, $\mu_n = 2\pi(n-1)d_y \sin(\theta)\sin(\phi)$ and $\mathbf{z}_n$ is the nth column of $\mathbf{Z}$.

In the following, we show that the RIP can be enforced if the 2D transmit array is symmetric horizontally and vertically (see Fig. 1) and the transmit weight matrix takes the following format [18]

$$\mathbf{W} = \begin{bmatrix} \mathbf{w}_{1,1} & \cdots & \mathbf{w}_{1,k'} & \tilde{\mathbf{w}}_{n,1}^* & \cdots & \tilde{\mathbf{w}}_{n,k'}^* \\ \mathbf{w}_{2,1} & \cdots & \mathbf{w}_{2,k'} & \tilde{\mathbf{w}}_{n-1,1}^* & \cdots & \tilde{\mathbf{w}}_{n-1,k'}^* \\ \vdots & \ddots & \vdots & \vdots & \ddots & \vdots \\ \mathbf{w}_{n,1} & \cdots & \mathbf{w}_{n,k'} & \tilde{\mathbf{w}}_{1,1}^* & \cdots & \tilde{\mathbf{w}}_{1,k'}^* \end{bmatrix} \tag{18}$$

where $k' = K/2$ and K is the arbitrary, but even, number of orthogonal waveforms, $\mathbf{w}_{n,k}$ is the vector of dimension $M_t \times 1$ that contains the subset of the weights in $\mathbf{w}_k$ associated with the nth column of the RCA, and $\tilde{\mathbf{w}}_{n,k}$ is the flipped version of $\mathbf{w}_{n,k}$. We will refer to the kth column of this matrix as $\mathbf{v}_k = [\mathbf{w}_{1,k}^T, \mathbf{w}_{2,k}^T, \cdots, \mathbf{w}_{n,k}^T]^T$. Similarly, we refer to the flipped conjugated version of $\check{\mathbf{v}}_k = [\tilde{\mathbf{w}}_{n,k}^H, \tilde{\mathbf{w}}_{n-1,k}^H, \ldots, \tilde{\mathbf{w}}_{1,k}^H]^T$. In order for the RIP to be enforced, the condition

$$|\mathbf{v}_k^H \mathbf{a}(\theta,\phi)| = |\check{\mathbf{v}}_k^H \mathbf{a}(\theta,\phi)|, \quad \theta \in [\frac{-\pi}{2}, \frac{\pi}{2}], \phi \in [0, 2\pi]. \tag{19}$$

must hold. If (19) holds, then the beam-patterns corresponding to the beam-space vectors $\mathbf{v}_k^H$ and $\check{\mathbf{v}}_k^H$ differ only in a phase rotation, which can be used for determining DOA. Expanding the inner-products in (19), we obtain

$$\begin{aligned} \mathbf{v}_k^H \mathbf{a}(\theta,\phi) &= \sum_{n=1}^{N_t} \mathbf{w}_{n,k}^H \mathbf{a}_n(\theta,\phi) \\ &= \sum_{n=1}^{N_t} (\mathbf{w}_{n,k}^T \mathbf{a}_n^*(\theta,\phi))^* \\ &= e^{j2\pi\xi(\theta,\phi)} \sum_{n=1}^{N_t} (\mathbf{w}_{n,k}^T \tilde{\mathbf{a}}_{N_t+1-n}(\theta,\phi))^* \\ &= e^{j2\pi\xi(\theta,\phi)} (\check{\mathbf{v}}_k^H \mathbf{a}(\theta,\phi))^* \end{aligned} \tag{20}$$

where $\xi = d_x(M_t - 1)\mu + d_y(N_t - 1)\zeta$, and $\mu = sin(\theta)cos(\phi)$ and $\zeta = sin(\theta)sin(\phi)$. It is clear that the two complex quantities $\mathbf{v}_k^H \mathbf{a}(\theta,\phi)$ and $\check{\mathbf{v}}_k^H \mathbf{a}(\theta,\phi)$ are equal in magnitude, but differ by a phase difference due to their conjugate relationship and the phase term $e^{j2\pi d_x(M_t-1)\mu} e^{j2\pi d_y(N_t-1)\zeta}$. Symmetric sparsity in the transmit antenna array does not affect the equality in (19). Thus, the RIP is enforced by the structure in (18) and this difference in phases can be used to enable the use of search-free direction finding techniques at the receive array.

IV. Simulation Results

In our simulations, we assume an 7×7 URA with $d_x = d_y = \lambda/2$ where λ is the wavelength. In the first example, the mainlobe of the desired 2D transmit beampattern is defined by $\Theta = [30°, 50°]$ and $\Phi = [70°, 110°]$. We allow for a transition zone of width $10°$ at each side of the mainlobe in the elevation domain and of width $20°$ at each side of the mainlobe in the azimuth domain. The remaining areas of the elevation and azimuth domains are assumed to be a stopband region. We use the general optimization toolbox CVX to solve the optimization problem (14)–(16). We use $K = 4$ transmit beams to focus the transmit energy within the desired 2D spatial sector.

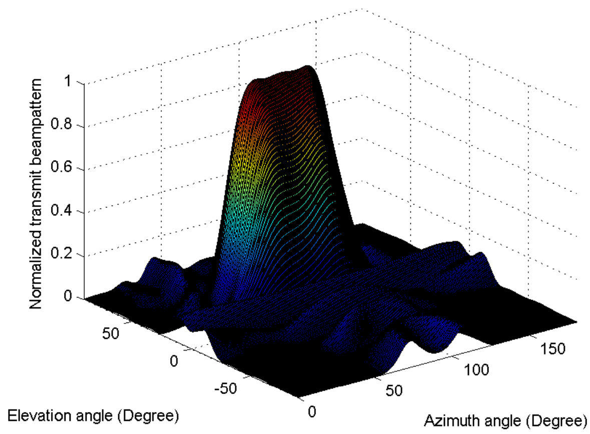

Fig. 2. Example 1: Normalized 2D transmit beampattern.

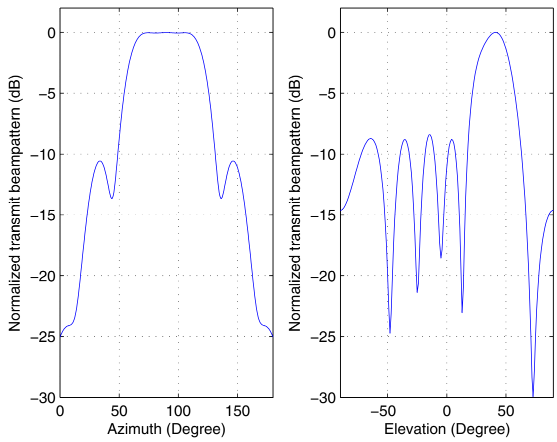

Fig. 3. Example 1: Azimuth and elevation cross sections of the normalized transmit beampattern calculated at $\theta = 40°$ and $\phi = 90°$, respectively.

The overall 2D transmit beampattern obtained by solving (14)–(16) is shown in Fig. 2. The overall beampattern before and after applying randomization remain almost the same. It can be seen from the figure that the transmit power is focused within the desired 2D sector. If needed, additional constraints can be easily imposed in (14)–(16) to keep the sidelobes below a certain level. Fig. 3 shows two cross sections of the 2D beampattern. The first cross section (left side of the figure) is plotted versus the azimuth angle, holding the elevation angle θ constant at $40°$ while the second cross section (right side of the figure) is plotted versus the elevation angle, holding the azimuth angle θ constant at $90°$. As we can see in that figure, the transmit power is concentrated in the desired azimuthal and elevation sectors.

In the second example, we compare the target localization performance of the proposed 2D transmit beamforming based MIMO radar to the performance of the conventional MIMO radar. For the conventional MIMO radar, M_tN_t orthogonal harmonics of unit energy are used. Each transmit antenna is used for omni-directional radiation of one of the M_tN_t orthogonal waveforms. While for the 2D transmit beamforming based MIMO radar, $K = 4$ orthogonal waveforms are used. Each waveform is radiated over one of the four transmit beams designed in the previous example. The transmit weight vectors are scaled such that the total transmit energy is M_tN_t. Two narrowband targets are assumed to be located in the far-field at the azimuth directions $\phi_1 = 90°$ and $\phi_2 = 95°$ and the elevation directions $\theta_1 = 38°$ and $\theta_2 = 42°$, respectively. The receive array of $M_r = 8$ elements is chosen. The locations of the receive antennas in a Cartesian 2D space are chosen randomly. The x- and y-components of the location of each receive antenna is drawn uniformly from the set $[0, \ 4\lambda]$. The sample covariance matrix for both methods considered is calculated based on 100 snapshots. The signal and noise subspaces for both methods is calculated using eigen decomposition. A signal-to-noise ratio (SNR) of 5 dB is used. The MUSIC algorithm is used for target localization. Fig. 4 shows the 2D MUSIC spectrum for the conventional MIMO radar. Fig. 5 shows the projections of the 2D MUSIC spectrum for the conventional MIMO radar onto the azimuth (top) and elevation (bottom) domains, respectively. It is clear from the two figures that the MUSIC spectrum for conventional MIMO radar is barely capable of resolving the two targets. It is observed through simulations that the MUSIC spectrum for SNR values below 0 dB fails to resolve the two targets. Fig. 6 shows the 2D MUSIC spectrum for the proposed 2D transmit beamforming based MIMO radar. Fig. 7 shows the projections of the 2D MUSIC spectrum for the 2D transmit beamforming based MIMO radar onto the azimuth (top) and elevation (bottom) domains, respectively. It is clear from the two figures that the proposed 2D transmit beamforming based MIMO radar has much better localization capabilities as compared to the conventional MIMO radar. It is observed during simulations that the 2D transmit beamforming based MIMO radar is cabable of resolving the two targets for SNR values below -10 dB. Other examples that that show the performance versus SNR and that employs the RIP of the proposed method will be given in the journal version of the paper.

It is worth noting that the size of the virtual data associated with the conventional MIMO radar is $M_tN_tM_r \times 1$ while the size of the virtual data associated with the 2D transmit beamforming based MIMO radar is $KM_r \times 1$. Therefore, the computational complexity of computing the signal and noise subspaces associated of the conventional MIMO radar will be of $O(M_t^3N_t^3M_r^3)$ while the computational complexity of computing the signal and noise subspaces associated of the 2D transmit beamforming based MIMO radar will be of $O(K^3M_r^3)$. This shows that the proposed 2D transmit beamforming based MIMO radar is also advantageous over the conventional MIMO radar in terms of the required computational load.

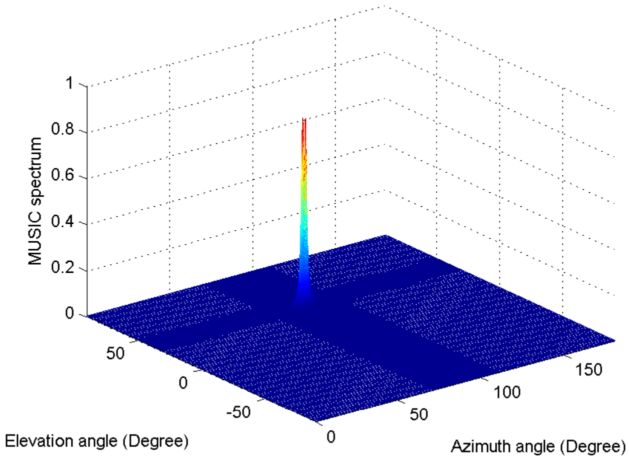

Fig. 4. Example 2: 2D MUSIC spectrum for conventional MIMO radar.

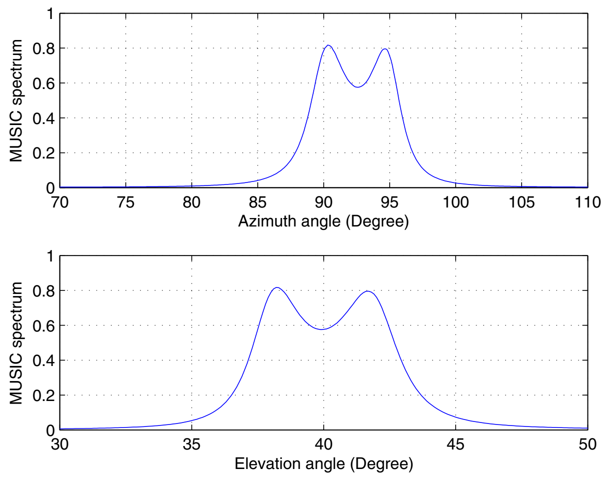

Fig. 5. Example 2: MUSIC spectrum for conventional MIMO radar projected onto the azimuth (top) and elevation (bottom) axes.

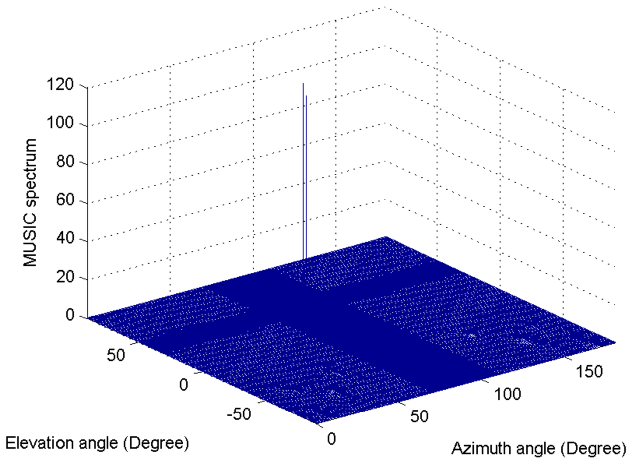

Fig. 6. Example 2: 2D MUSIC spectrum for MIMO radar with 2D transmit beamforming.

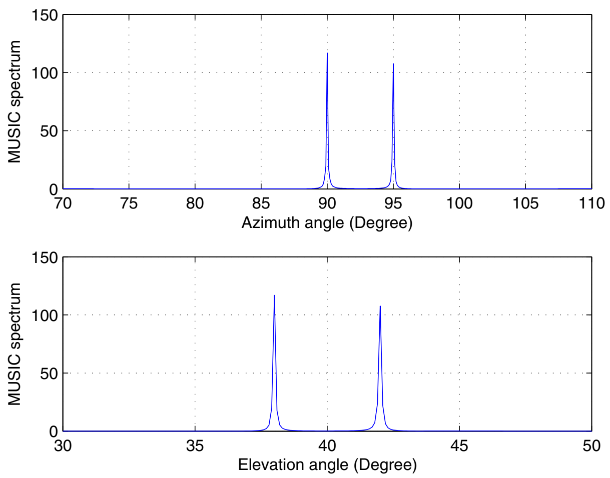

Fig. 7. Example 2: MUSIC spectrum for MIMO radar with 2D transmit beamforming projected onto the azimuth (top) and elevation (bottom) axes.

V. Conclusion

The problem of 2D transmit beamforming design for MIMO radar with 2D planar arrays with missing elements has been addressed. We have formulated the 2D transmit beamforming design problem as an optimization problem that minimizes the difference between a 2D desired transmit beampattern and the actual one given in (6) while satisfying constraints such as uniform transmit power across the array elements, sidelobe level control, etc. Moreover, different transmit beams can be enforced to have rotational invariance with respect to each other, a property that enables efficient computationally cheap 2D direction finding at the receiver. Semi-definite relaxation is used to recast the optimization problem as a convex one that can be solved efficiently using the interior point methods. It has been shown that the proposed method for 2D transmit beamforming improves the localization performance at lower computational burden as compared to the conventional MIMO radar. Simulation examples are used to validate the proposed 2D transmit beamforming design method.

Acknowledgment

The authors would like to thank Samsung Thales Co., Ltd., Chang-Li 304, Namsa-Myun, Cheoin-Gu, Yongin-City, Gyeonggi-D, Korea, for the financial support.

References

[1] J. Li and P. Stoica, *MIMO Radar Signal Processing*. New Jersy: Wiley, 2009.

[2] A. Haimovich, R. Blum, and L. Cimini, “MIMO radar with widely separated antennas,” *IEEE Signal Processing Magaz.*, vol. 25, pp. 116–129, Jan. 2008.

[3] J. Li and P. Stoica, “MIMO radar with colocated antennas,” *IEEE Signal Processing Magaz.*, vol. 24, pp. 106–114, Sept. 2007.

[4] E. Fishler, A. Haimovich, R. Blum, L. Cimini, D. Chizhik, and R. Valenzuela, “Spatial diversity in radarsModels and detection performance,” *IEEE Trans. Signal Process.*, vol. 54, pp. 823–838, Mar. 2006.

[5] A. Hassanien, S. A. Vorobyov, and A. B. Gershman, “Moving target parameters estimation in non-coherent MIMO radar systems,” *IEEE Trans. Signal Processing*, vol. 60, no. 5, pp. 2354–2361, May 2012.

[6] A. Hassanien and S. A. Vorobyov, “Phased-MIMO radar: A tradeoff between phased-array and MIMO radars,” *IEEE Trans. Signal Processing*, vol. 58, no. 6, pp. 3137–3151, June 2010.

[7] D. Wilcox and M. Sellathurai, “On MIMO Radar Subarrayed Transmit Beamforming,” *IEEE Trans. Signal Processing*, vol. 60, no. 4, pp. 2076–2081, Apr. 2012

[8] A. Hassanien and S. A. Vorobyov, “Transmit energy focusing for DOA estimation in MIMO radar with colocated antennas,” *IEEE Trans. Signal Processing*, vol. 59, no. 6, pp. 2669–2682, June 2011.

[9] T. Aittomaki and V. Koivunen, “Beampattern optimization by minimization of quartic polynomial,” in Proc. *15 IEEE/SP Statist. Signal Process. Workshop*, Cardiff, U.K., Sep. 2009, pp. 437-440.

[10] D. Fuhrmann and G. San Antonio, “Transmit beamforming for MIMO radar systems using signal cross-correlation,” *IEEE Trans. Aerospace and Electronic Systems*, vol. 44, no. 1, pp. 1–16, Jan. 2008.

[11] A. Hassanien and S. A. Vorobyov, “Direction finding for MIMO radar with colocated antennas using transmit beamspace preprocessing,” in *Proc. IEEE Inter. Workshop Computational Advances in Multi-Sensor Adaptive Processing*, Aruba, Dutch Antilles, Dec. 2009, pp. 181–184.

[12] P. Stoica, J. Li, and Y. Xie, “On probing signal design for MIMO radar,” *IEEE Trans. Signal Process.*, vol. 55, no. 8, pp. 4151–4161, Aug. 2007.

[13] A. Khabbazibasmenj, S. A. Vorobyov, and A. Hassanien, “Transmit beamspace design for direction finding in colocated MIMO radar with arbitrary receive array,” in *Proc. 36th ICASSP*, Prague, Czech Republic, May 2011, pp. 2784–2787.

[14] A. Khabbazibasmenj, S. A. Vorobyov, and A. Hassanien, “Robust adaptive beamforming via estimating steering vector based on semidefinite relaxation,” in *Proc. 44th ASILOMAR*, Pacific Grove, California, USA, Nov. 2010, pp. 1102–1106.

[15] A. Khabbazibasmenj, S. A. Vorobyov, and A. Hassanien, “Robust adaptive beamforming based on steering vector estimation with as little as possible prior information,” *IEEE Trans. Signal Processing*, vol. 60, no. 6, pp. 2974–2987, June 2012.

[16] Z.-Q. Luo, W.-K. Ma, A. M.-C. So, Y. Ye, and S. Zhang, “Semidefinite relaxation of quadratic optimization problems,” *IEEE Signal Processing Magaz.*, vol. 27, no. 3, pp. 20–34, May 2010.

[17] K. T. Phan, S. A. Vorobyov, N. D. Sidiropoulos, and C. Tellambura, “Spectrum sharing in wireless networks via QoS-aware secondary multicast beamforming,” *IEEE Trans. Signal Processing*, vol. 57, no. 6, pp. 2323–2335, June 2009.

[18] A. Khabbazibasmenj, S. A. Vorobyov, A. Hassanien, and M. W. Morency, “Transmit beamspace design for direction finding in colocated MIMO radar with arbitrary receive array and even number of waveforms,” in *Proc 46th Annual Asilomar Conf. Signals, Systems, and Computers*, Pacific Grove, California, USA, Nov. 4–7, 2012.